JOURNAL OF NEUROPHYSIOLOGY
Vol. 76, No. 1, July 1996. *Printed in U.S.A.*

Development of BK Channels in Neocortical Pyramidal Neurons

JIAN KANG, JOHN R. HUGUENARD, AND DAVID A. PRINCE
Department of Neurology and Neurological Sciences, Stanford University, Stanford, California 94305

SUMMARY AND CONCLUSIONS

1. Postnatal development of a large conductance Ca^{2+}-activated K^+ channel (BK channel) was investigated in neocortical infragranular pyramidal neurons with inside-out and outside-out patch-clamp configurations. Neurons were acutely isolated from slices of 1- to 28-day-old rats (*P1–P28*) by using a vibrating glass probe after preincubation with low concentrations of enzymes. Patch membrane area was estimated by measuring membrane capacitance. The density, distribution, voltage dependence, Ca^{2+} sensitivity, kinetics, and pharmacological properties of BK channels were examined in neurons from animals of different ages.

2. In somata, the density of BK channels was 0.056 ± 0.011/μm^2 in P1 neurons and 0.312 ± 0.008/μm^2 in *P28* neurons. There was an abrupt increase between *P5* and *P7* at a rate of ~0.042/μm^2/day. Before *P5* and after *P7*, the density of BK channels also increased but at slower rates.

3. The density of BK channels in proximal apical dendrites underwent a similar developmental sequence. There was a relatively large increase between *P5* and *P7* with a rate of ~0.021/μm^2/day, and after *P7*, channel density increased more slowly (~0.002/μm^2/day). In *P1* neurons, channel density in apical dendrites was 0.039 ± 0.008/μm^2, which was close to that in somata, whereas in *P28* neurons, channel density (0.134 ± 0.008/μm^2) was less than one-half of that in somata.

4. The distribution of BK channels was different in immature and mature neurons. In somata of *P1* neurons, BK channels were distributed singly without evidence of clustering, whereas in *P28* neurons BK channels were clustered in groups of ~4.

5. BK channels in both *P1* and *P14* neurons showed a steep increase in the probability of opening (P_o) as intracellular Ca^{2+} concentration was raised from 50 to 100 nM, especially at positive membrane potentials. The Ca^{2+} dependence, as measured by the $[Ca^{2+}]_i$ that provided half-maximal P_o at a variety of membrane potentials, was not different in patches from *P1* and *P14* neurons. On the other hand, the voltage dependence of BK channels shifted during ontogeny such that P_o was larger at negative potentials in *P14* than in *P1* neurons.

6. The voltage dependence of *P1* BK channels was bimodally distributed with 57% of channels exhibiting an "immature" pattern consisting of a more positive $V_{1/2}$ and a smaller change in voltage required to produce an *e*-fold increase in P_o. Immature type *P1* BK channels showed a longer mean closed time at negative membrane potentials than either *P14* or "mature" *P1* BK channels.

7. No postnatal developmental changes in pharmacological properties of BK channels were observed. In both mature and immature neurons, BK channels were partially inhibited by 30 or 100 nM charybdotoxin (ChTX) and fully blocked by 1 μM ChTX. The IC_{50} for ChTX was 100 nM, indicating that BK channels in neocortical pyramidal neurons are much less sensitive to ChTX than those in muscle cells and sympathetic ganglion neurons. BK channels were also inhibited by 0.5 mM tetraethylammonium chloride (TEA) and 50 μM trifluoperazine.

8. These data indicate that functional somatic and dendritic BK channels are inserted into neuronal membranes during neocortical development, with an especially rapid increment in density occurring around *P5–P7*. These changes, which occur at a time when other voltage-gated ion channels are known to be increasing in density, contribute to the development of neocortical excitability.

INTRODUCTION

Pyramidal neurons of the cerebral cortex undergo remarkable changes in their electrophysiological properties during postnatal development. Immature neocortical and other central neurons generate action potentials (APs) that have a smaller peak amplitude, longer duration, and slower rise and fall rate (Huguenard et al. 1988; Kriegstein et al. 1987; McCormick and Prince 1987). The most reasonable explanation for these results is that ion channels in the neuronal membrane are differentially expressed in immature and mature neurons. Ca^{2+}-activated K^+ channels (K_{Ca}) are widely distributed in a variety of animal cells including neurons (Adams et al. 1982; Hermann and Hartung 1983; Lancaster et al. 1991; Meech 1972, 1978; Yoshida et al. 1991), muscle (Benham et al. 1985; Blatz and Magleby 1986; Latorre et al. 1982; Pallota et al. 1981; Walsh and Singer 1983), and gland cells (Cook et al. 1984; Marty 1981, 1989). In neurons, K_{Ca} channels have been reported to play important roles in regulating various AP-related parameters including AP duration, AP repolarization, afterhyperpolarization (AHP) (Brown et al. 1983; Hotson and Prince 1980; Lancaster and Nicoll 1987; Storm 1987), interspike interval, firing rate and pattern, and burst termination (Lancaster and Nicoll 1987; Lang and Ritchie 1987). At least three types of K_{Ca} channels have been described (Castle et al. 1989; Reinhart et al. 1989) including a large conductance (BK), a small conductance (SK), and an intermediate conductance channel (IK). The large conductance of neuronal BK channels allows them to play an important role in hyperpolarizing the membrane potential when they are activated. Although a late emergence of Ca^{2+} sensitivity in BK channels has been reported in embryonic amphibian cultures (Blair and Dionne 1985), postnatal developmental changes in density and properties of mammalian BK channels have not received attention.

BK channels are voltage dependent; however, previous studies from a variety of preparations have reported a wide range of open probabilities (P_o) at the resting potential (Lancaster et al. 1991; Trautman and Marty 1984; Wann and Richards 1994). In hippocampal cultures prepared from *postnatal day 3–4* (*P3–P4*) rats (Wann and Richards 1994), the activity of BK channels at the resting potential was much higher than that of BK channels in similar cultures from *E17–E18* embryonic rats (Lancaster et al. 1991). It remains to be determined whether there are developmental changes in voltage dependence of BK channels. In the pres-

ent study, we used a vibrating glass microprobe (Vorobjev 1991) and treatment with low concentrations of enzymes to isolate deep layer pyramidal neurons from neocortical slices of *P1–P28* rats. Inside-out and outside-out patch-clamp configurations were used to investigate the density, voltage dependence, Ca^{2+} sensitivity, kinetics, and pharmacological properties of BK channels. We found that the density of BK channels increased during postnatal development, with an abrupt increase between *P5* and *P7*. Voltage-dependent activation of BK channels showed heterogeneity in *P1* neurons, and about one-half of the channels were activated at more depolarized potentials than in mature cells.

METHODS

Dissociation of neurons

Brain slices were first prepared using previously described techniques (Huguenard et al. 1988). Sprague-Dawley rats of either sex (Simonsen Breeders) were anesthetized with pentobarbital sodium (55 mg/kg) and decapitated. The brain was rapidly removed, a block of tissue dissected and glued to the stage of a vibratome (TPI, St. Louis, MO), and three or four 300-μm coronal slices containing sensorimotor cortex were cut. Slices were incubated at 37°C for 20 min in piperazine-*N,N'*-bis(2-ethanesulfonic acid) (PIPES) buffer solution (see *Solutions*) gassed with 100% O_2, and containing protease XXIII (0.10–0.15 mg/ml, Sigma) and collagenase (0.10–0.15 mg/ml, Worthington Biochemical, Freehold, NJ). These low concentrations of enzymes were used because preliminary experiments showed that concentrations >0.5 mg/ml markedly affected the voltage dependence and Ca^{2+} sensitivity of BK channels in young, but not older animals. Voltage dependence of channel opening was shifted to depolarized levels, and there was less sensitivity to Ca^{2+} in patches when these high enzyme concentrations were used (unpublished observations). After incubation, slices were washed four times with standard slice perfusate (see *Solutions*). A 2- to 3-mm-wide block containing somatosensory cortex (cortical Par 1) (Paxinos and Watson 1986) was trimmed and put into a 3 ml poly-L-lysine precoated culture dish. Neurons were isolated with a vibrodissociation device similar to that described by Vorobjev (1991). The vibration was applied to the slice via a 60-mm-long pipette, tapered over 15 mm, made from a 1.5-mm-diam glass capillary. The tapering shank of the pipette was bent at a right angle, and a fire-polished glass bead was formed at the tip (0.3 mm diam). The pipette was fixed to the movable arm of a 12-V relay, and the vibration amplitude was adjusted via two small screws installed on the relay. The body of the relay was affixed to a manipulator to control the position of the vibrating probe. The rod, vibrating at 10 Hz, was touched to the cut edge of the slice near layer 5 and moved gradually into the slice along layer 5. The neurons being isolated from the slice by vibration were observed with an inverted microscope. Once a sufficient number of neurons were isolated, vibration was stopped, and the slice was removed. Neurons were allowed to settle down and attach to the dish for 5 min, and then perfusion was begun.

Single-channel recording

Single-channel activities were recorded at room temperature (21–22°C) with the use of outside-out and inside-out configurations of the patch-clamp technique (Hamill et al. 1981) and an Axopatch 200A amplifier (Axon Instruments, Burlingame, CA). Recording electrodes had resistances of 4–7 MΩ. Seal formation was monitored, and seals <1 GΩ in resistance were rejected. Outside-out patches were obtained by pulling off pipettes from neurons in whole cell configurations, and inside-out patches were excised by withdrawing pipettes away quickly from neurons in cell-attached configurations. The channel activity from inside-out patches was recorded during perfusion of the tip of the patch pipette with intracellular solutions containing different Ca^{2+} concentrations (see *Solutions*), using a multi-tube delivery system that allowed rapid solution changes. Signals were filtered through an 8-pole Bessel low-pass filter with 1–2 kHz cutoff frequency and stored on a videotape recorder via a NEURO-CORDER converter (NEURO-DATA Instrument) for later computer analysis. Signals triggered by ramp commands were directly recorded onto the computer hard disk with the use of the PCLAMP6.0-Clampex program. The term membrane potential refers to the potential difference between intracellular and extracellular sides of the membrane.

Measurement of capacitance and channel density

Channel recordings and patch capacitance were obtained by the methods illustrated in Fig. 1. A small positive pressure was applied to the patch pipette and released once the pipette touched a neuron, whereupon a slight negative pressure was applied to obtain a gigaohm seal. An inside-out patch was excised from the neuron, and the channel activity was measured. After finishing the measurement, the inside-out patch was lowered down close to the dish bottom, and the bath solution was reduced to a minimum. A square +1-mV, 2-ms pulse was delivered to the patch and the total capacitative current (I_C), consisting of the sum of pipette capacitance and membrane capacitance, was measured. A strong electrical pulse via the ZAP button on the Axopatch 200A was then used to rupture the patch, and a gigaohm seal again obtained by touching the pipette tip to the plastic dish bottom. The same square pulse was

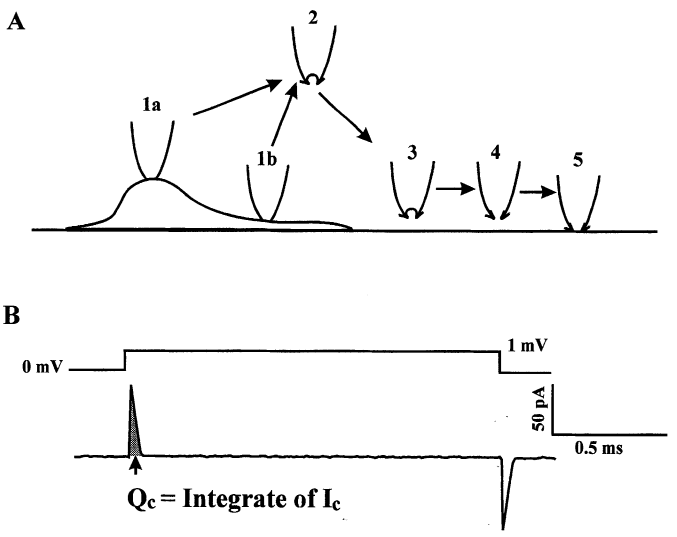

FIG. 1. Measurement of membrane capacitance. *A*: experimental sequence. 1, recording pipettes were brought into contact with the soma (1a) or dendrite (1b) of a neuron and a slight suction was applied to obtain a GΩ seal. 2, pipettes were pulled quickly from the neuron and an inside-out patch was excised. Single-channel activity was then recorded. 3, at the end of each recording, the pipette was lowered down as close as possible to the bottom of the chamber, and the bath solution was also reduced to as low a level as possible. A square pulse was delivered to the pipette, and the total capacitance (sum of the membrane capacitance and the pipette capacitance) was measured. 4, an electrical pulse (2–3 s, manual) via the ZAP button on the AXOPATCH 200A was applied to break the membrane in the patch. 5, the tip of the pipette was advanced so that it contacted the bottom of the plastic dish, and a gigaohm seal (>1 GΩ) was formed again. The same voltage step command was delivered to measure the pipette capacitance. The membrane capacitance was obtained by subtracting the pipette capacitance from the total capacitance. *B*: trace showing capacitance current (I_C) and calculation of capacitative charge (Q_C).

delivered to obtain the pipette capacitative current, which was subtracted from the total capacitative current to obtain the membrane capacitance. The integrate function in the PCLAMP6.0-Clampfit program was used to obtain the area of I_C (capacitative charge, Q_C), and capacitance was calculated with the use of the equation $C = Q_C/dV$, where dV is the voltage step. Data from 15 traces were averaged to obtain the capacitative current in each case. The membrane patch area was derived from its measured capacitance by assuming that the specific capacitance was close to 0.8 $\mu F/cm^2$ (Major et al. 1994). Channel density was calculated for each animal, rather than for each patch, using the equation $D = \Sigma(N)/\Sigma(A)$, where D is channel density, N is the number of channels in each patch, A is the area of each patch, and $\Sigma(N)$ and $\Sigma(A)$ are sums of N and A in each animal, respectively. The average rate of increase in channel density was calculated with the following equation: rate = $(D_x - D_y)/(x - y)$, where D_x and D_y are channel densities for neurons at ages of x and y days, respectively.

Solutions

The intracellular solution contained (in mM) 130 KCl, 5 ethylene glycol-bis(β-aminoethyl ether)-*N,N,N′,N′*-tetraacetic acid (EGTA), 2 $MgCl_2$, 10 *N*-2-hydroxyethylpiperazine-*N′*-2-ethanesulfonic acid (HEPES), and 4 dextrose (pH adjusted to 7.2 with KOH). Estimated final $[K^+]$ was 140 mM after adding KOH to adjust pH. Calcium-free solution containing 5 mM EGTA was assumed to have 3–5 nM free Ca^{2+}. Free calcium levels in EGTA buffer were calculated on the basis of pH, [Mg], [Ca], and [EGTA]. Free $[Ca^{2+}]$ of 0.05 and 0.1, 0.5, 1, and 10 μM were obtained by adding a total of 0.86, 2.47, 2.50, 2.96, and 2.99 mM of $CaCl_2$, respectively, to a 5 mM EGTA and 2 mM Mg^{2+}-containing solution (Stockbridge 1987). The extracellular solution (standard slice perfusate) contained (in mM) 126 NaCl, 5 KCl, 1.25 NaH_2PO_4, 2 $MgCl_2$, 2 $CaCl_2$, 10 glucose, and 26 $NaHCO_3$, pH 7.4 when gassed with 95% O_2-5% CO_2. When recording from outside-out patches, pipettes contained the intracellular solution plus 1 mM ATP and 2.5 mM $CaCl_2$ (free Ca^{2+} = 0.5 μM in 5 mM EGTA), and standard extracellular solution was perfused. For inside-out patches, pipettes contained the standard intracellular solution (Ca^{2+} free) and the perfused solution contained either the standard intracellular solution (symmetric $[K^+]$; $[K^+]_o/[K^+]_i$ = 140/140 mM) or the standard extracellular perfusate ($[K^+]_o/[K^+]_i$ = 140/5 mM). The PIPES buffer solution used for acute dissociations contained (in mM) 120 NaCl, 5 KCl, 1 $CaCl_2$, 1 $MgCl_2$, 1 pyruvic acid, 25 dextrose, and 20 PIPES (pH adjusted to 7.2 with NaOH).

Charybdotoxin, dipotassium adenosine triphosphate (ATP), HEPES, trifluoperazine, poly-L-lysine, tetraethylammonium chloride monohydrate (TEA), and EGTA were purchased from Sigma. Other chemicals were purchased from Mallinckrodt Specialty Chemicals (Paris, Kentucky).

Data analysis

PCLAMP6.0 was used to plot raw current traces, the probability of channel opening (P_o), amplitude histograms, and open time and closed time histograms. Current responses to voltage ramps were leak subtracted via PCLAMP6.0-Clampfit program, and leak resistances were estimated from current traces without channel activities. Single-channel currents were sampled every 50 μs with PCLAMP6.0-Fetchex and analyzed with Fetchan. A 50% threshold criterion was used to determine the durations of open and closed events. The collected open and closed intervals were binned with PCLAMP6.0-Pstat, and logarithmic distributions of open and closed durations were exponentially fitted with the use of the Maximal Likelihood method. The binwidth was automatically determined with Pstat.

RESULTS

Changes in the density of BK channels during postnatal development

Inside-out patches were excised from somata and apical dendrites of presumed pyramidal neurons. Cells selected for study had a single large apical dendrite and an oblong soma. Where possible, several patches were obtained from the same neuron. A total of 396 BK channels was examined in 218 inside-out patches excised from isolated pyramidal neurons, of which 298 channels were recorded in 173 somatic patches, and 98 channels in 45 dendritic patches. BK channels had a conductance of 181.6 ± 3.9 (SE) pS in symmetric K^+ concentrations (n = 21, membrane potentials of −20, −40, −60, and −80 mV) and showed bursts or clusters of channel openings. There was no difference in conductance between BK channels from *P14* and *P1* neurons (*P1*: 183.2 ± 6.4 pS, n = 10; and *P14*: 179.8 ± 4.4 pS, n = 11). Rectification of BK channels was observed in recordings of responses to ramp voltage commands (Fig. 2, *A* and *B*) as previously reported (Kang et al. 1994). In a minority of somatic patches (n = 14, 8.1%), we also found a 30-pS K_{Ca} channel.

BK channels in neocortical cells were similar to those in other neurons in that they were voltage dependent, highly selective to K^+, and sensitive to intracellular Ca^{2+}. Recordings during steady holding potentials and ramp voltage commands both showed that the frequency of openings was voltage dependent, with fewer openings occurring as membrane was hyperpolarized and more openings during depolarization (Fig. 2, *A* and *B*). When the solution bathing the intracellular side of the patch was changed from a low K^+-high Na^+ (5 mM K^+ and 140 mM Na^+) to a high K^+-low Na^+ solution (140 mM K^+ and 0 mM Na^+), the reversal potential shifted from +61.5 ± 1.1 mV to −0.4 ± 1.5 mV (n = 27; note shift in intersection of dashed lines with closed state baselines in traces of Fig. 2, *A* and *B2–B4*). According to the Goldman-Hodgkin-Katz relationship, the calculated ratio of K^+ to Na^+ permeability was greater than 15:1. Bathing the intracellular side of inside-out patches with solutions containing 100 nM or higher $[Ca^{2+}]$ triggered significant increases in BK channel openings (Fig. 2*B*), showing the Ca^{2+} dependence of the channel.

Recordings of responses to ramp voltage commands in asymmetric K^+ concentrations (intracellular 5 mM and extracellular 140 mM with 2 mM Ca^{2+}) clearly showed the numbers of BK channels in each patch, because channels were largely open during the initial membrane depolarization and then closed as the membrane was hyperpolarized (Fig. 2*A*). For example, in the recording of Fig. 2*A* (*left*), a patch excised from a *P1* neuron contained only one channel, whereas the patch from a *P28* neuron of Fig. 2*A* (*right*) had five BK channels. Recordings of responses to ramp voltage commands were thus useful for counting channel numbers in adult neurons where multiple channels were present in each patch. Although the difference in channel density could also be observed with symmetric K^+ (Fig. 2*B*), the exact number of channels in patches containing multiple channels was not as clear as in asymmetric K^+ concentrations (e.g., 100 nM Ca^{2+} trace of Fig. 2*B3, right*).

To compare expression levels of BK channels during post-

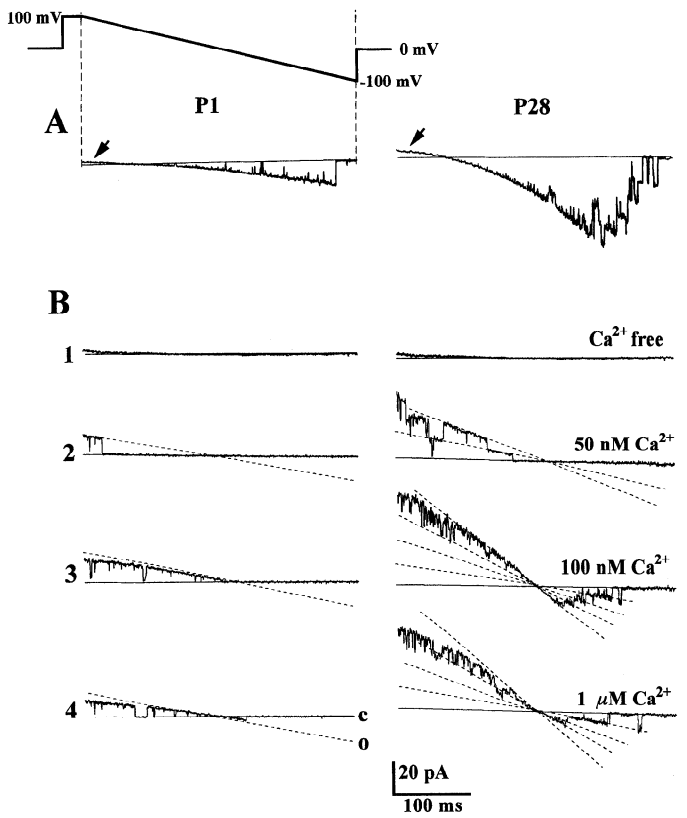

FIG. 2. Recordings of responses of Ca^{2+}-activated K^+ channels (BK channels) to ramp voltage commands (*top*). Voltage values refer to membrane potentials. V_h = 0 mV. *Left* and *right columns* are inside-out patch recordings from *P1* and *P28* neurons, respectively. Current segments were taken from the beginning to just before the end of voltage ramps. Current recordings and ramp commands are on the same time scale. Current trace reflects response to the ramp portion of the voltage command as shown by the vertical dashed lines in *A, P1*. Data were leak subtracted so that any deviation from the closed status (horizontal solid line) denotes channel openings. Dashed and solid lines indicate open (**o**) and closed (**c**) states, respectively. *A*: recordings obtained when the pipette solution contained 140 mM KCl, and the bath solution contained 5 mM KCl and 2 mM $CaCl_2$. Rectification was very strong at positive voltages (arrows). *B*: recordings with the symmetric (140 mM) K^+ solutions containing nominally Ca^{2+}-free (*1*), 0.05 (*2*), 0.1 (*3*), and 1 μM [Ca^{2+}] (*4*). Each dashed line in *B2–B4* was drawn by hand to indicate a well-defined open status. Single-channel openings are shown in *P1* patch of *B2–B4;* 2 channels in *B2, P28;* and 4 channels in *B3* and *B4, P28.* Recordings of *P28* channel activities in *A* and *B* were from different patches and *B1–B4* were from the same patch.

natal development, channel density from neurons of different ages was measured. Channel density was obtained by dividing channel number by the membrane area, which was obtained by measuring membrane capacitance as described in METHODS. Table 1 shows the patch membrane capacitances from somata and dendrites in the different age groups. Values for patch membrane capacitance (and hence patch area) were larger in dendrites, perhaps because stronger suction was often needed to obtain a gigaohm seal. Because BK channels may not be distributed evenly across the neuronal membrane, channel density was calculated by averaging results from all somatic or dendritic patches for each animal as a unit, rather than from each patch. The mean density of BK channels in somatic membrane was 0.056 ± 0.011/μm^2 in *P1* and 0.312 ± 0.008/μm^2 in *P28* neurons (Table 2). From *P1* to *P5,* BK channel density increased slowly, followed by an abrupt increase between *P5* and *P7* at a rate of 0.042/μm^2/day (Fig. 3). After *P7,* the density of channels continued to increase, but at a slower rate of 0.007/μm^2/day (Fig. 3). The average rate of increase from *P1* to *P28* was 0.008/μm^2/day. The median number of channels per patch also increased gradually with age (Fig. 4, *A–D*). The relationships between the channel number and the patch area are shown in Fig. 4, *E–H.* In *P1* neurons there were either no channels or one in almost every patch regardless of the patch area; in *P28* neurons the median number of channels per patch was four. If channels are distributed evenly across membrane, the channel number per patch should be proportional to the patch area, whereas a lack of correlation between these variables would indicate a nonuniform channel distribution, as might occur if channels were arranged in clusters. Linear regression of channel number versus patch area demonstrated little correlation between these variables ($r^2 \ll 0.01$) in *P1* neurons, probably because channels were too sparse to measure density per patch reliably. In *P6* and *P14* neurons, channel density was weakly correlated with membrane area ($r^2 \approx 0.3–0.5$), suggesting an even distribution at this stage. However, in *P28* neurons there was no correlation between channel number and patch area ($r^2 \ll 0.01$), and each patch contained about four, indicating apparent clustering. The results suggest that, in immature neurons, BK channels are evenly distributed in the neuronal membrane without clustering, whereas in mature neurons channels are clustered in groups of approximately four.

The density of BK channels in the proximal portion of primary apical dendrites of pyramidal neurons at different ages was also investigated. Patches were excised at a mean distance of 18 ± 2.6 μm from the soma-apical dendritic junction. From *P1* to *P5* only a small increase in the density of BK channels was observed in these dendritic patches (Fig. 3). The mean density of BK channels in apical dendrites (0.039 ± 0.008/μm^2) was not significantly different from that in somata during this period (Table 2). As in somatic membranes, during *P5–P7* an abrupt increase in the density of BK channels occurred in apical dendrites, although the rate of increase (0.021/μm^2/day) was not as large as for somata (0.042/μm^2/day). After *P7,* channel densities in apical dendrites increased very slowly at a rate of 0.002/μm^2/day (Fig. 3). The average rate of increase in dendritic channel density from *P1* to *P28* was 0.003 μm^{-2}/day, which is lower than that in somata (0.008 μm^{-2}/day). Channel densities in apical dendrites were significantly lower than in somata in *P7, P14,* and *P28* animals ($P < 0.01$; Fig. 3).

Changes in voltage dependence and Ca^{2+} sensitivity of BK channels during postnatal development

Because patches from *P28* neurons often contained multiple channels (e.g., Fig. 2), it was difficult to calculate open probability (P_o) for each channel at this age. Recordings of responses to ramp voltage commands showed that BK channels from *P14* and *P28* neurons had a similar voltage dependence; therefore voltage dependence was investigated by comparing the open probability-voltage (P_o vs. V) relationships of BK channels from *P1* neurons with that from *P14* neurons. Transitions in channel state were measured over 4 s for each voltage by the PCLAMP6.0-Fetchan pro-

TABLE 1. *Membrane capacitance in patches*

	P1	*P3*	*P5*	*P7*	*P14*	*P28*
From somata	100 ± 31	105 ± 39	71 ± 14	70 ± 14*	135 ± 32	100 ± 20*
Number of animals	3	1	2	2	4	5
Number of patches	12	6	7	10	15	23
From dendrites	157 ± 34		162 ± 55	186 ± 42	157 ± 45	187 ± 35
Number of animals	2		2	2	3	4
Number of patches	5		9	16	11	7
Pipette capacitance			3,954 ± 64			

Capacitance values are means ± SE expressed in fF. *P1, postnatal day 1.* * $P < 0.05$ compared with dendrites at the same age (Student's *t*-test).

gram, and P_o was determined over this period by using PCLAMP-Pstat program. P_o-V curves showed that in both *P1* and *P14* neurons, BK channels could open with strong depolarization at a very low $[Ca^{2+}]$ (0.05 μM and below; points with solid circles (●) in Fig. 5, *A* and *B*), although P_o was much smaller than with higher $[Ca^{2+}]$s. As $[Ca^{2+}]$ was increased, the P_o-V curves shifted to the left; however, the shift in voltage was insensitive to $[Ca^{2+}]$ values greater than 0.5 μM (Fig. 5, *A* and *B*). With $[Ca^{2+}]$s of 0.5, 1 (Fig. 5*C*), and 10 μM, P_o of BK channels in *P14* neurons was significantly larger than in *P1* neurons at membrane potentials of −20, −40, and −60 mV. At more depolarized membrane potentials (+20 to +80 mV), BK channels in both *P1* and *P14* neurons exhibited long-lasting openings; however, at negative membrane potentials (−20 to −60 mV), more openings were seen in patches from *P14* than from *P1* neurons (Fig. 5*D*). To further analyze the changes in voltage dependence during development, individual P_o-V curves were fitted by the Boltzmann equation $P_o = P_{o,max}/\{P_{o,max} + \exp[(1/K)(V_{1/2} - V)\}$. The equation was transformed into the logarithmic form, $V = V_{1/2} + K \cdot \ln \{P_o/[P_{o,max}(1 - P_o)]\}$, where K is the membrane depolarization for an *e*-fold increase in P_o, and $V_{1/2}$ is the patch potential at which P_o is one-half of the maximum P_o ($P_{o,max}$). $V_{1/2}$ and K were obtained by plotting $\ln \{P_o/[P_{o,max}(1 - P_o)]\}$ against voltage (Fig. 6*A*). The mean value of $V_{1/2}$ in *P1* neurons was more positive, and K was smaller than that in *P14* neurons (Table 3). Further analysis showed that $V_{1/2}$ had a normal Gaussian distribution in *P14* neurons, with a mean, mode, and median all near −13 mV (Fig. 6*B* and Table 3), whereas in *P1* neurons $V_{1/2}$ distribution had two peaks with median values of −13.1 and +11.6 mV (Fig. 6*C*). Fifty-seven percent (13/23) of BK channels in *P1* neurons had $V_{1/2}$ values outside of the 95% confident range for $V_{1/2}$ of BK channels in *P14* neurons (−12.7 ± 16.8 mV). These results indicate that about one-half of BK channels in early postnatal neurons are immature and require stronger depolarization for activation than mature channels. During the first few postnatal weeks, neuronal BK channels become functionally mature.

Ca^{2+} sensitivity of BK channels in *P1* and *P14* neurons was analyzed by plotting the P_o versus $[Ca^{2+}]$ relationships. BK channels in both *P1* and *P14* neurons showed a remarkable increase in P_o as $[Ca^{2+}]$ was raised from 50 to 100 nM, especially at positive potentials (Fig. 7, *A* and *B*). P_o values in *P14* neurons were higher than those in *P1* neurons at membrane potentials of −20, −40, or −60 mV (Fig. 7*C*). However, activation curves obtained by plotting percent of maximal P_o against $[Ca^{2+}]$ were similar for BK channels in *P1* and *P14* neurons (Fig. 7*D*), indicating that differences between channels at these ages reflected alternations in voltage dependence, rather than Ca^{2+} sensitivity.

Changes in kinetics of BK channels during postnatal development

Kinetic analysis of BK channels was obtained from patches in which single-channel activities were observed. Data were derived from three groups of BK channels: *P14,* immature *P1,* and mature *P1* (Fig. 8). A *P1* BK channel with a $V_{1/2}$ that fell outside the 95% confident range of $V_{1/2}$ for *P14* BK channels (e.g., Fig. 6*C*) was defined as an immature BK channel. Although BK channels exhibited a burst property, especially with membrane potentials positive to −20 mV, a burst duration analysis across the whole voltage range was precluded because channels would burst continuously above +20 mV and not burst at all below −60 mV. Therefore conventional open time and closed time analysis was applied to the data. The open duration distribution could be fit well by a single exponential function (Fig. 8, *A–C*), whereas the closed duration distribution required a double exponential for a satisfactory fit at all ages (Fig. 8, *D–F*). For example, at a holding potential of −40 mV, *P14,* immature *P1,* and mature *P1* BK channels showed a similar open duration distribution (Fig. 8, *A–C*). The mean open times (τ_o) for *P14,* immature *P1,* and mature *P1* were 5.5 ± 1.4 ms, 4.6 ± 1.0 ms, and 4.1 ± 1.3 ms, respectively. The fast closed time distributions (τ_{c1}) were also similar in all groups. But the slow closed duration distribution for immature *P1* BK channels (Fig. 8*F;* τ_{c2} = 75.4 ± 20 ms) was different from that for *P14* (Fig. 8*D;* τ_{c2} = 11.3 ± 2.8 ms) or mature *P1* (Fig. 8*E;* τ_{c2} = 8.7 ± 1.2 ms) channels.

TABLE 2. *The density of BK channels in somata and apical dendrites*

	P1	*P3*	*P5*	*P7*	*P14*	*P28*
Somata	0.056 ± 0.011	0.058 ± 0.007	0.079 ± 0.009*	0.163 ± 0.026*,†	0.229 ± 0.014*,†	0.312 ± 0.008*,†
Dendrites	0.039 ± 0.008		0.059 ± 0.006*	0.100 ± 0.022*	0.113 ± 0.014*	0.134 ± 0.008*

Values are means ± SE expressed in number/μm^2. Numbers of patches and animals were the same as indicated in legend of Fig. 3. BK channels, Ca^{2+}-activated K^+ channels; *P1, postnatal day 1.* * $P < 0.01$ compared with *P1* (Student's *t*-test). † $P < 0.01$ compared with dendrites at the same age.

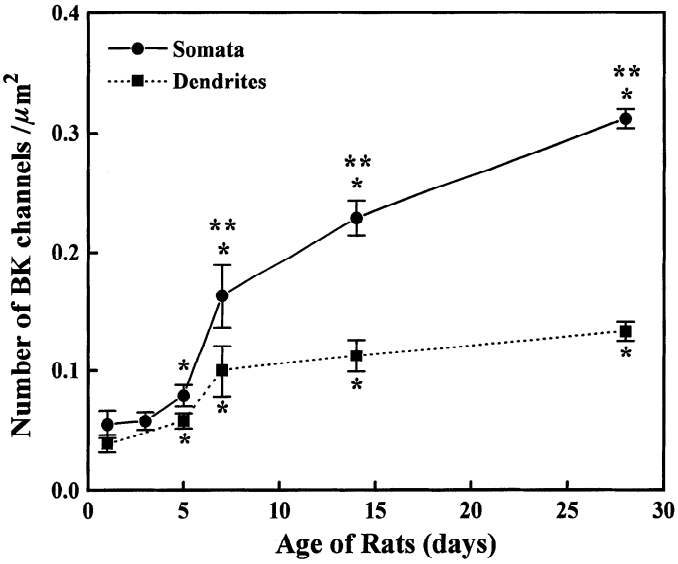

FIG. 3. Changes in BK channel density during postnatal development. Channel density was calculated by dividing the channel number by the patch membrane area (see METHODS). Data are means ± SE. Numbers of samples from somata were 30, 17, 30, 29, 31, and 33 patches from 4 *P1*, 3 *P3*, 5 *P5*, 4 *P7*, 5 *P14*, and 4 *P28* animals, respectively. Samples from dendrites numbered 8, 8, 12, 11, and 6 patches from 3 *P1*, 3 *P5*, 4 *P7*, 4 *P14*, and 3 *P28* animals, respectively. $*P < 0.01$ compared with *P1*. $**P < 0.01$ compared with dendrites at the same age.

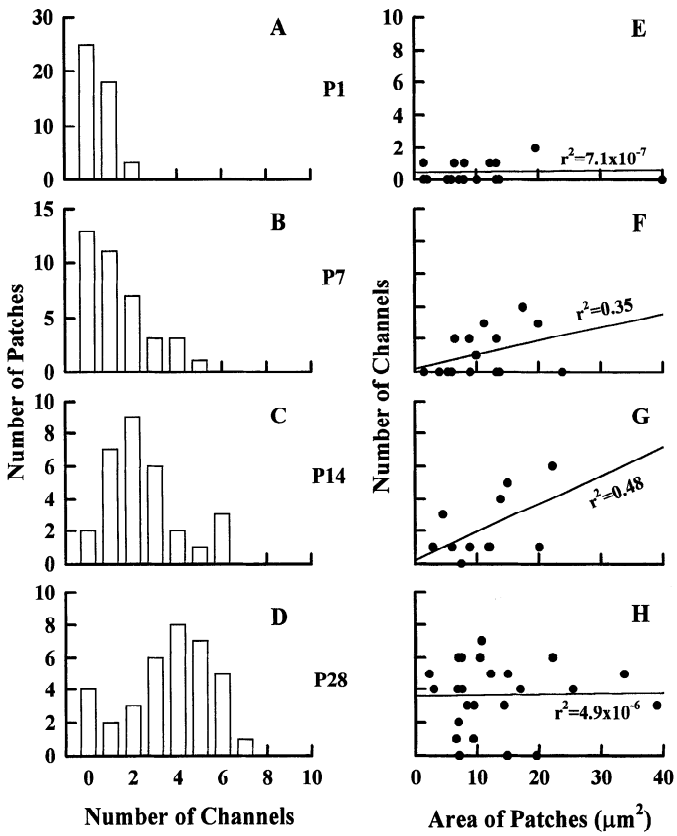

FIG. 4. Distribution of BK channels. *A–D*: distribution of channels/patch for *P1*, *P7*, *P14*, and *P28* rats, respectively. *E–H*: numbers of channels in each patch vs. patch membrane area for *P1*, *P7*, *P14*, and *P28* rats, respectively. Lines in *E–H* are linear regressions for all points, including those patches without channel activity. Scale values for number of channels in *E* for *E–H*.

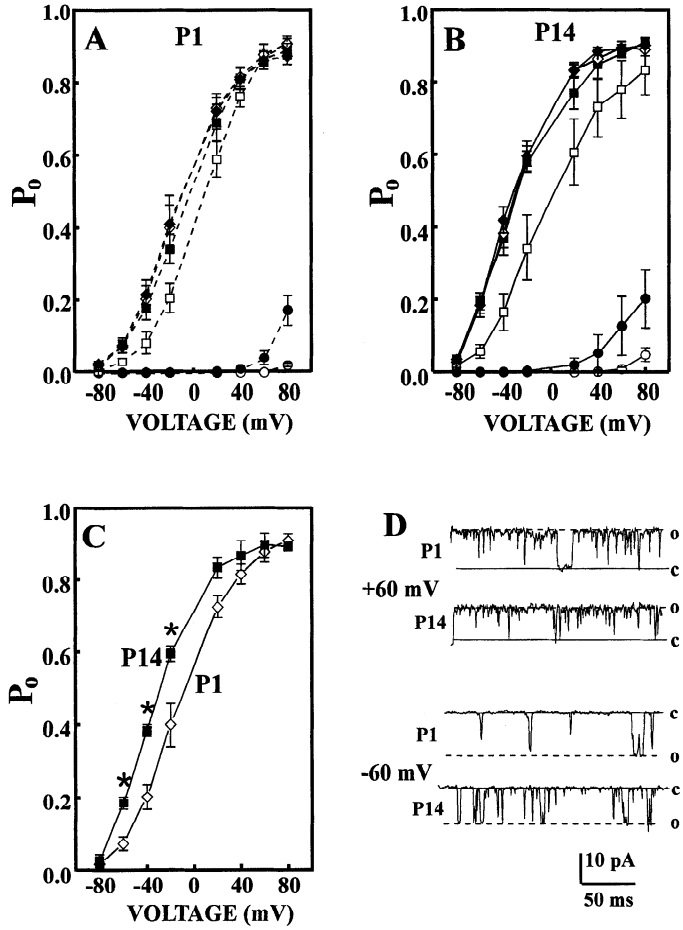

FIG. 5. Voltage dependence of BK channels in *P1* and *P14* neurons. *A*: open probability vs. voltage relationship (P_o-V) for BK channels in inside-out patches from *P1* neurons during exposure to solutions containing various Ca^{2+} concentrations: nominally Ca^{2+}-free (○), 0.05 μM (●), 0.1 μM (□), 0.5 μM (■), 1 μM (◇), and 10 μM (♦). $n = 13$ channels. *B*: P_o-V curves for BK channels in inside-out patches from *P14* neurons. Symbols as in *A*. $n = 10$ channels. *C*: P_o-V curves for BK channels in inside-out patches from *P1* (◇) and *P14* (♦) neurons in 1 μM Ca^{2+} solution. Data are from *A* and *B*. $*P < 0.05$ compared with *P1* neurons. *D*: recordings of BK channel activity at holding potentials of +60 and −60 mV in *P1* and *P14* neurons. Solid lines indicate closed state (**c**), and dashed lines indicate open state (**o**). Downward deflections represent inward currents. Data in *A–C* are means ± SE.

The voltage dependence of open and closed times was examined for *P14*, mature *P1*, and immature *P1* BK channels. The mean open time (τ_o) versus voltage relationships showed that the values of the mean open time in these three subgroups of BK channels were not different across the voltage range of −60 to +60 mV (Fig. 9*A*). The shorter time constant (τ_{c1}) for fitting the closed duration distributions

TABLE 3. *Values of $V_{1/2}$ and K in P1 and P14 neurons*

	$V_{1/2}$, mV	*K*, mV	*n*
P1	3.5 ± 3.2*	22.3 ± 0.6†	23
P14	−12.7 ± 1.8	26.2 ± 1.0	22

Values are means ± SE. $V_{1/2}$, holding potential when P_o was ½ of $P_{o,max}$; *K*, change in voltage required to produce an *e*-fold increase in P_o; *P1*, *postnatal day 1*. $*P < 0.01$ compared with 14 days. $†P < 0.05$ compared with 14 days.

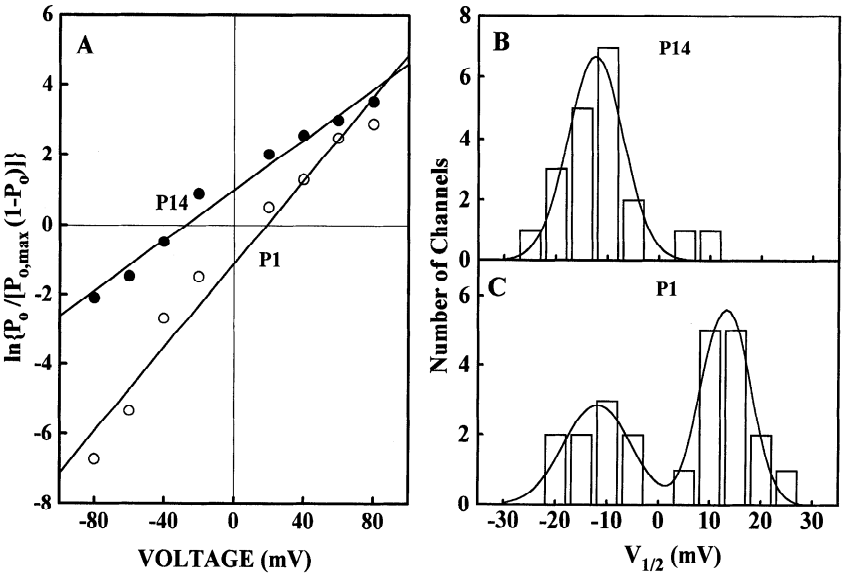

FIG. 6. Distributions of $V_{1/2}$ for BK channels in inside-out patches from *P1* and *P14* neurons. *A*: logarithmic Boltzmann fittings of P_o-V curves for representative single immature *P1* (○) and *P14* BK channels (●). *B* and *C*: distributions of $V_{1/2}$ for BK channels from *P14* (*B*) and *P1* neurons (*C*). Lines in *B* and *C* are Gaussian fits. Data in *B* and *C* are from patches perfused with solutions containing either 0.5 or 1 μM Ca^{2+}, and binwidth was 5 mV.

roughly corresponded to the intraburst closures and was not significantly different among *P14*, mature *P1*, and immature *P1* groups (Fig. 9*B*). The longer closed time constant (τ_{c2}), which represented the interburst closures, was significantly different between immature *P1* and *P14* or mature *P1* groups especially at negative membrane potentials ($P < 0.05$; Fig. 9*C*). No significant difference in τ_{c2} was observed between *P14* and mature *P1* groups.

Pharmacological properties of BK channels in neocortical pyramidal neurons

The effects of charybdotoxin (ChTX) were tested using outside-out and inside-out patch configurations. When perfused over five outside-out patches, 30 and 100 nM ChTX only partially inhibited, and 1 μM ChTX completely blocked BK channel openings in the same patches (Fig. 10*A*). Thirty and 100 nM ChTX reduced P_o of BK channels to 82.5 ± 3.1% and 51.6 ± 3.2% of control values ($n = 5$), respectively. Based on results from this limited number of patches, the concentration of ChTX that produced a 50% blockade (IC_{50}) was close to 100 nM in both *P1* ($n = 2$) and *P14* ($n = 3$) neurons. With ChTX in the pipette solution (1 μM), BK channels of inside-out patches were also inhibited (Fig. 10*B*; $n = 5$). Pipette tips were filled with the standard intracellular solution and backfilled with ChTX-containing solution, so that channel openings were present initially, and then blocked as ChTX diffused from the shank into the electrode tip. Perfusion of 0.5 mM TEA-containing solution inhibited BK channel openings in outside-out patches in both *P14* ($n = 4$) and *P1* ($n = 2$) neurons (Fig. 10*C*). The effects of TEA appeared as a reduction in unitary current amplitude, presumably because TEA blocks and unblocks the channel with very fast kinetics not resolvable by the recording system (Benham et al. 1985; Reinhart et al. 1989; Yellen 1984). When perfused over inside-out patches, trifluoperazine (50 μM), a phenothiazine derivative, also blocked BK channel activities in both *P14* ($n = 3$) and *P1* ($n = 2$) neurons (Fig. 10*D*) in a pattern similar to that reported by Ikemoto et al. (1992).

DISCUSSION

Before discussing the principal findings of these experiments, it is important to highlight two technical factors that might have affected the results. As mentioned in METHODS, when concentrations of protease XXIII and collagenase >0.5 mg/ml were used to obtain dissociated neurons, there were marked selective effects on both voltage dependence and Ca^{2+} sensitivity of BK channels in young, but not older animals. These differences, presumably due to alterations in channel proteins by the enzymes, disappeared when lower concentrations were used. Although it is well known that various enzymes used for cell dissociation can affect channel functions (Hestrin and Korenbrot 1987), to our knowledge the developmental selectivity encountered here has not been reported and should be taken as a caution in studies employing acutely dissociated neurons to examine age-related differences in properties of agonist gated or voltage-dependent channels. The properties of BK channels in dissociated cells exposed to the low enzyme concentrations reported here are similar to those we have found recently in inside-out patches excised from pyramidal neurons in neocortical slices (Kang et al. 1995) studied under enzyme-free conditions, suggesting that this factor did not influence the present results.

A second important technical issue is the measurement of the patch membrane capacitance, which was critical to obtaining reliable patch area and therefore channel density. Because the membrane capacitance is only a small fraction of the pipette capacitance (Table 1), a subtraction method is necessary to obtain the former. Several findings suggest that estimates of patch membrane capacitances (and therefore areas) in this study were accurate: *1*) these data agree with those of patch area obtained microscopically by others (Sakmann and Neher 1983); *2*) effective pipette sealing (>1 GΩ) was obtained by touching the bottom of the dish, which made for valid capacitance measurements; and *3*) as expected, values for patch area were similar in different age groups (Table 1).

The BK channels we obtained in acutely isolated neocorti-

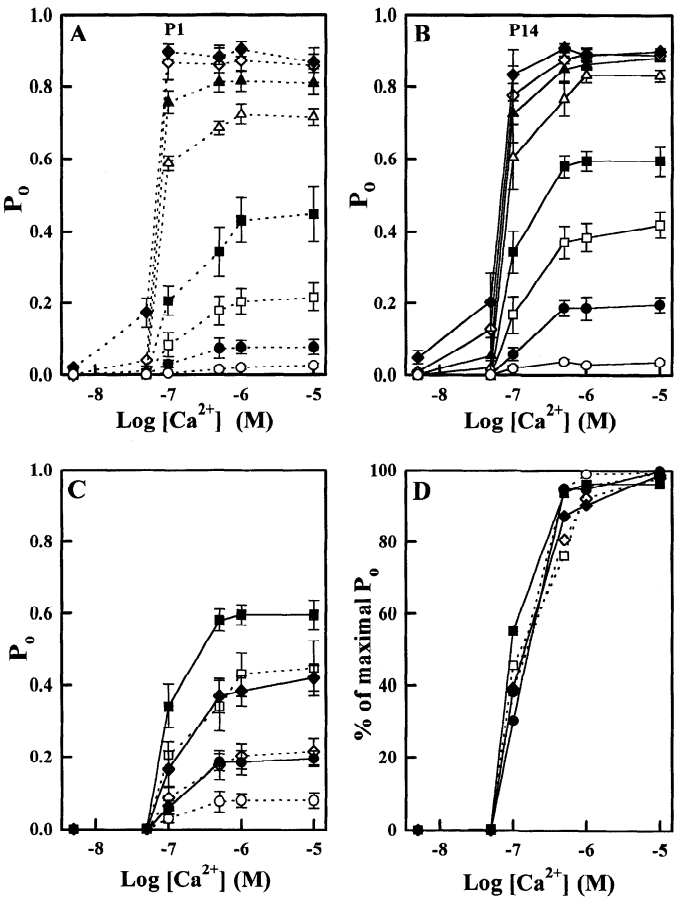

FIG. 7. Ca^{2+} sensitivity of BK channels in *P1* and *P14* neurons. Inside-out patches were perfused with solutions containing different [Ca^{2+}]s. *A*: activation of BK channels by Ca^{2+} in *P1* neurons at holding potentials of −80 mV (○), −60 mV (●), −40 mV (□), −20 mV (■), +20 mV (△), +40 mV (▲), +60 mV (◇), and +80 mV (◆). n = 13 channels. *B*: activation of BK channels by Ca^{2+} in *P14* neurons at different holding potentials. Symbols as in *A*. n = 10 channels. *C*: from data of *A* and *B*. Activation of BK channels by Ca^{2+} in *P1* (□, ◇, and ○) and *P14* (■, ◆, and ●) neurons at holding potentials of −60 mV (● and ○), −40 mV (◆ and ◇), and −20 mV (■ and □). *D*: data in *C* plotted as a percentage of each maximal P_o (P_{max}). Symbols as in *C*. Data in *A–C* are means ± SE.

cal pyramidal cells have properties similar to those previously reported in other neurons (Ikemoto et al. 1992; Lancaster et al. 1991; Reinhart et al. 1989; Wann and Richards 1994), including *1*) high selectivity for K^+ over Na^+ with a P_K/P_{Na} ratio >15; *2*) a threshold for activation by Ca^{2+} of 100 nM at positive membrane potentials; *3*) a conductance of 181 pS in symmetric K^+ solution (140/140 mM); *4*) voltage dependence, with an open probability that increased *e*-fold for a 22- to 26-mV depolarization of membrane potential; and *5*) inhibition by extracellular 0.5 mM TEA, and intracellular 50 μM trifluoperazine. BK channels in neocortical pyramidal neurons have less sensitivity to ChTX than those in muscle cells and sympathetic ganglion neurons, as will be discussed below. The developmental time course of changes in BK channel density closely resembles that reported for Na^+ channels and some K^+ channels (Hamill et al. 1991; Huguenard et al. 1988; McCormick and Prince 1987), in that there is a sudden increase in density beginning at about *P5–P7*. BK channel densities in somata and proximal apical dendrites were similar and increased slowly before *P5;* however, after *P7,* apical dendrites had a lower channel density than somata.

Voltage dependence has been used to predict whether BK channels can open when neurons are in the resting state (i.e., at membrane potentials of approximately −70 mV). Previous studies addressing this issue have led to conflicting results. Lancaster et al. (1991) used *E17–E18* rat pups to prepare cell cultures and obtained BK channels without openings at −70 mV, whereas Wann and Richards (1994) reported a P_o of 0.45 at −70 mV in cultures from *P3–P4* rat pups and inferred that the difference between their results and those of Lancaster et al. was due to the different ages of animals used to prepare cultures. Our results in newborn rats (*P1*) show that some BK channels (57%) are still immature in terms of voltage dependence, have a more positive $V_{1/2}$, and are not active at −70 mV, as reported by Lancaster et al. (1991). However, "mature" BK channels that have a more negative $V_{1/2}$ and are active at −70 mV are also present (Wann and Richards 1994). The kinetic analysis also showed that immature BK channels had a longer mean closed time at negative membrane potentials, which reflects fewer openings. Heterogeneity of BK channels has also been observed by other investigators in embryonic rat telencephalon (Bulan et al. 1994). The causes for these variations in channel properties in immature neurons require further examination. Studies of variants of *Slowpoke,* a *Drosophila* large conductance K^+ channel expressed in oocytes, have indicated that alternate splicing of a common RNA precursor produces functional diversity of the expressed channel properties of conductance, Ca^{2+} sensitivity, and kinetics (Lagrutta et al. 1994). These results in *Drosophila* suggest that one explanation for the heterogeneity of BK channels that we found in immature neocortical neurons may be alternate splicing.

In contrast to the above age-related alterations in voltage-dependent properties, the responses of BK channels to Ca^{2+} and pharmacological agents do not appear to change during development. Calcium sensitivity is a critical property of BK channels that affects their physiological function in neurons by determining the intracellular Ca^{2+} level required for channel opening. Under the conditions of our experiments, the approximate threshold for activation of BK channels was a Ca^{2+} concentration of 100 nM. Although BK channels undergo developmental changes in Ca^{2+} sensitivity in cultured spinal neurons of *Xenopus* (Blair and Dionne 1985), we did not find similar postnatal alterations in cortical pyramidal neurons. Likewise, BK channel ChTX sensitivity was similar in neurons of different ages. ChTX, a peptide toxin from *Leiurus quinquestriatus* venom, produces a specific high affinity blockade (IC_{50} = 3 nM) of BK channels in muscle cells and sympathetic ganglion neurons (Castle et al. 1989). On the other hand, a BK channel in posterior pituitary nerve terminals is reportedly insensitive to ChTX (Bielefeldt and Jackson 1993). By incorporating rat cortical plasma membrane vesicles into planar lipid bilayers, Reinhart et al. (1989) also observed a BK channel insensitive to 10 nM ChTX. In the present study, 50% blockade of BK channels in outside-out patches required 100 nM ChTX, and complete blockade occurred only with 1 μM ChTX, indicating that the BK channels in neocortical pyramidal neurons are less sensitive to ChTX than those in muscle

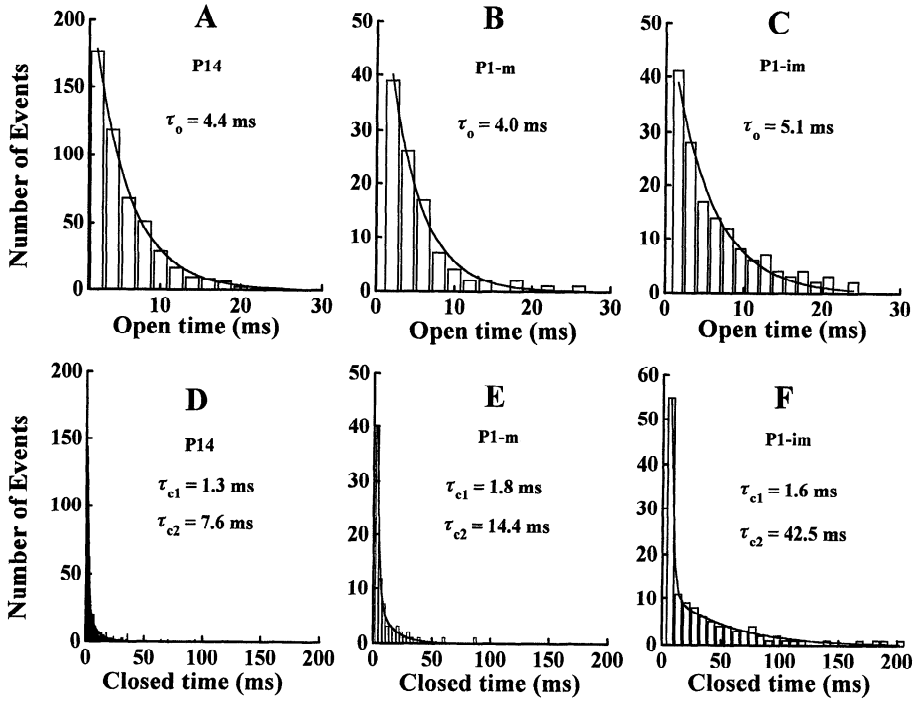

FIG. 8. Distributions of open time and closed time of BK channels. *A–C*: open duration distribution histograms for a *P14* BK channel, a mature *P1* BK channel (*P1*-m), and an immature *P1* BK channel (*P1*-im), respectively. *D–F*: closed duration distribution histograms for the channels in *A–C*. V_h = −40 mV; $[Ca^{2+}]$ = 1 μM for *A–F*. Lines are exponential fittings. Open time (*A–C*) and closed time (*D–F*) duration distributions are fitted by 1 and 2 exponentials, respectively.

cells and sympathetic ganglion neurons, perhaps providing further support for the possibility that there are functional subtypes of BK channels.

The decreased density, more positive $V_{1/2}$ and longer mean closed time at negative membrane potentials that characterize BK channels in immature animals would all tend to make channels less influential in affecting membrane excitability. It should be noted that the maturation of Ca^{2+} channels, Ca^{2+} buffer systems, and intracellular modulatory enzymes for BK channels may also influence functions of these channels during development. BK channels have been hypothesized to contribute to the fast AHP in hippocampal pyramidal neurons, based on the blockade of the fast AHP and consequent spike broadening produced by ChTX and low concentrations of TEA (Lancaster and Nicoll 1987; Storm 1987). However, as yet there is no evidence for such a role in neocortical neurons. If BK channels do contribute to the conductances that repolarize the action potential, then decreased density and maturational immaturity would contribute (along with decreased Na^+ channel density) to the broader spikes that characterize immature neocortical pyramidal neurons (Kriegstein et al. 1987; McCormick and Prince 1987). A relatively lower density of dendritic BK channels might also be implicated in the slower time course of dendritic spikes reported in hippocampal (Wong et al. 1979) and cortical pyramidal neurons (Kim and Connors 1993). Recently we obtained recordings of action potentials and simultaneous channel activity from neocortical pyrami-

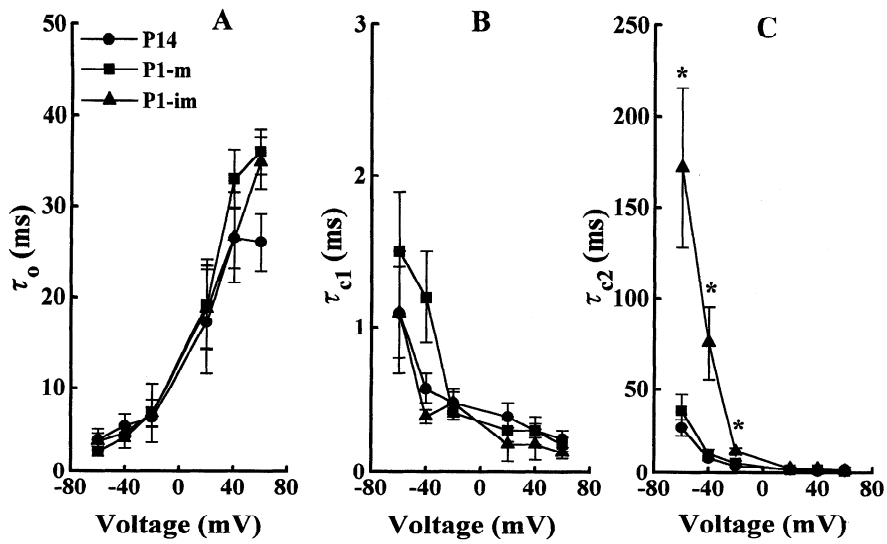

FIG. 9. Kinetics of BK channels in *P1* and *P14* neurons. *A*: mean open time (τ_o)-voltage relationships for *P14*, mature *P1* (*P1*-m), and immature *P1* (*P1*-im) BK channels (n = 5). *B*: τ_{c1}-V curves for *P14*, mature *P1*, and immature *P1* BK channels (n = 5). *C*: τ_{c2}-V curves for *P14*, mature *P1*, and immature *P1* BK channels. *P < 0.05 compared with *P14* and mature *P1* channels (n = 5). To derive τ_{c1} and τ_{c2}, the closed time distributions were fitted with 2 exponentials; τ_{c1} was the shorter and τ_{c2} the longer time constant. Symbols in *B* and *C* as in *A*.

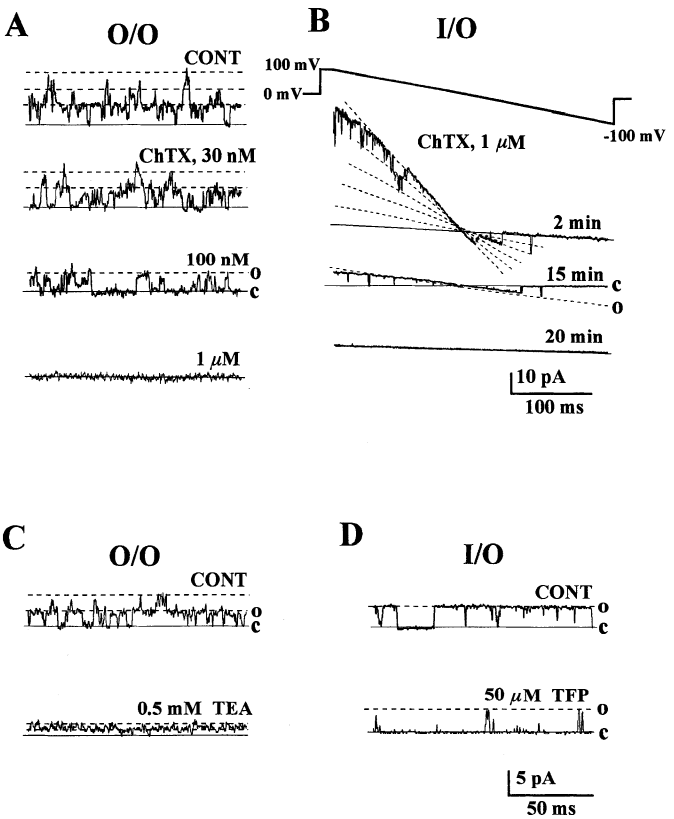

FIG. 10. Pharmacological properties of BK channels. *A*: inhibitory effect of charybdotoxin (ChTX) on BK channels in an outside-out patch (O/O) from a *P14* neuron. V_h = 0 mV. The pipette solution contained 0.5 μM Ca^{2+}. The control solution (CONT) and solutions containing 30 nM, 100 nM, or 1 μM of ChTX were perfused. *B*: inhibitory effect of ChTX on BK channels in an inside-out patch (I/O) from a *P14* neuron. ChTX solution (1 μM) was used to backfill the pipette. Traces are recordings of responses to a ramp voltage command (*top*) 1 min, 15 min, and 20 min after the patch was excised from the neuron. The bath solution contained 0.5 μM Ca^{2+}. *C*: effect of tetraethylammonium chloride monohydrate (TEA) on BK channels in an outside-out patch from a *P1* neuron. V_h = 0 mV. The pipette solution containing 0.5 μM Ca^{2+} and 0.5 mM TEA was applied in the bath solution. *D*: inhibitory effect of trifluoperazine (TFP) on a BK channel in an inside-out patch from a *P1* neuron. V_h = +40 mV. The control (CONT) bath solution contained 0.5 μM Ca^{2+}. TFP (50 μM) was applied in the bath solution. Calibrations in *D* for *A, C,* and *D*. Solid lines indicate the closed state (**c**), and dashed lines indicate the open state (**o**).

dal neurons in slices and found that BK channels did not open following single spikes or trains of 5–20 spikes, but only as neurons were deteriorating (Kang et al. 1995), raising the interesting possibility that the BK channel is activated as an "emergency" mechanism. The failure of channels to open in relation to single spikes or trains would seem to contradict the finding that the threshold concentration of Ca^{2+} for channel activation is 100 nM (Fig. 7), a value for $[Ca^{2+}]_i$ that would presumably be exceeded during such neuronal activity (Connor 1986; Connor et al. 1987). One possible explanation for this discrepancy might be the presence of intracellular enzymes that normally inhibit channel activation (Reinhart et al. 1991; Bielefeldt and Jackson 1994; Lee et al. 1995) and are not present in cell-free patches or deteriorated neurons. The finding that some neuromodulators regulate these enzymes (White et al. 1991) would make BK channels a potential target for modification by such agents.

Address for reprint requests: J. Kang, Dept. of Neurology and Neurological Sciences, Rm. M022, SUMC, Stanford University, Stanford, CA 94305.

Received 27 October 1995; accepted in final form 3 January 1996.

REFERENCES

ADAMS, P. R., CONSTANTI, A., BROWN, D. D., AND CLARK, R. B. Intracellular Ca^{2+} activates a fast voltage-sensitive K^+ current in vertebrate sympathetic neurons. *Nature Lond.* 246: 746–749, 1982.

BENHAM, C. D., BOLTON, T. B., LANG, K. J., AND TAKEWAKI, T. The mechanisms of action of Ba^{2+} and TEA on single Ca^{2+}-activated K^+ channels in arterial and intestinal smooth muscle cell membrane. *Pfluegers Arch.* 403: 120–127, 1985.

BIELEFELDT, K. AND JACKSON, M. B. A calcium-activated potassium channel causes frequency-dependent action-potential failures in a mammalian nerve terminal. *J. Neurophysiol.* 70: 284–298, 1993.

BIELEFELDT, K. AND JACKSON, M. B. Phosphorylation and dephosphorylation modulate a Ca^{2+}-activated K^+ channel in rat peptidergic nerve terminals. *J. Physiol. Lond.* 475: 241–254, 1994.

BLAIR, L. A. C. AND DIONNE, V. E. Developmental acquisition of Ca^{2+}-sensitivity by K^+ channels in spinal neurons. *Nature Lond.* 315: 329–330, 1985.

BLATZ, L. A. AND MAGLEBY, K. L. Single apamin-blocked Ca-activated K^+ channels of small conductance in cultured rat skeletal muscle. *Nature Lond.* 323: 718–720, 1986.

BROWN, D. A., CONSTANTI, A., AND ADAMS, P. R. Ca-activated potassium current in vertebrate sympathetic neurons. *Cell Calcium* 4: 407–420, 1983.

BULAN, E. J., BARKER, J. L., AND MIENVILLE, J. M. Immature maxi-K channels exhibit heterogeneous properties in the embryonic rat telencephalon. *Dev. Neurosci.* 16: 25–33, 1994.

CASTLE, N. A., HAYLETT, D. G., AND JENKINSON, D. H. Toxins in the characterization of potassium channels. *Trends Neurosci.* 12: 59–65, 1989.

CONNOR, J. A. Digital imaging of free calcium changes and of spatial gradients in growing processes in single, mammalian central nervous system cells. *Proc. Natl. Acad. Sci. USA* 83: 6179–6183, 1986.

CONNOR, J. A., TSENG, H. Y., AND HOCKBERGER, P. E. Depolarization- and transmitter-induced changes in intracellular Ca^{2+} of rat cerebellar granule cells in explant cultures. *J. Neurosci.* 7: 1384–1400, 1987.

COOK, D. L., IKEUCHI, M., AND FUYIMOTO, D. W. Lowering of pH inhibits Ca^{2+}-activated K^+ channels in pancreatic β-cells. *Nature Lond.* 311: 269–271, 1984.

HAMILL, O. P., HUGUENARD, J. R., AND PRINCE, D. A. Patch-clamp studies of voltage-gated currents in identified neurons of the rat cerebral cortex. *Cereb. Cortex* 1: 48–61, 1991.

HAMILL, O. P., MARTY, A., NEHER, E., SACKMANN, B., AND SIGWORTH, B. J. Improved patch-clamp techniques for high-resolution current recording from cells and cell-free membrane patches. *Pfluegers Arch.* 391: 85–100, 1981.

HERMANN, A. AND HARTUNG, K. Ca-activated K conductance in molluscan neurons. *Cell Calcium* 4: 387–405, 1983.

HESTRIN, S. AND KORENBROT, J. I. Voltage-activated potassium channels in the plasma membrane of rod outer segments: a possible effect of enzymetic cell dissociation. *J. Neurosci.* 7: 3072–3080, 1987.

HOTSON, J. R. AND PRINCE, D. A. A Ca-activated hyperpolarization follows repetitive firing in hippocampal neurons. *J. Neurophysiol.* 43: 409–419, 1980.

HUGUENARD, J. R., HAMILL, O. P., AND PRINCE, D. A. Development changes in Na^+ conductances in rat neocortical neurons: appearance of a slowly inactivating component. *J. Neurophysiol.* 59: 778–794, 1988.

IKEMOTO, Y., YOSHIDA, A., AND ODA, M. Blockade by trifluoperazine of a Ca^{2+}-activated K^+ channel in rat hippocampal pyramidal neurons. *Eur. J. Pharmacol.* 216: 191–198, 1992.

KANG, J., HUGUENARD, J. R., AND PRINCE, D. A. Ca^{2+}-activated potassium channels underlying afterhyperpolarization in neocortical pyramidal neurons. *Soc. Neurosci. 25th Annu. Meeting Abstr.* 718.16: 1826, 1995.

KANG, J., POSNER, P., AND SUMNERS, C. Calcium-modulated inward rectification of a calcium- activated potassium channel in cultured neurons. *J. Neurophysiol.* 72: 3023–3025, 1994.

KIM, H. G. AND CONNORS, B. W. Apical dendrites of the neocortex: correlation between sodium- and calcium-dependent spiking and pyramidal cell morphology. *J. Neurosci.* 13: 5301–5311, 1993.

KRIEGSTEIN, A. R., SUPPES, T., AND PRINCE, D. A. Cellular and synaptic physiology and epileptogenesis of developing rat neocortical neurons in vitro. *Dev. Brain Res.* 34: 161–171, 1987.

LAGRUTTA, A., SHEN, K. Z., NORTH, R. A., AND ADELMAN, J. P. Functional differences among alternatively spliced variants of slowpoke, a *Drosophila* calcium-activated potassium channel. *J. Biol. Chem.* 269: 20347–20351, 1994.

LANCASTER, B. AND NICOLL, R. A. Properties of two calcium-activated hyperpolarizations in rat hippocampal neurons. *J. Physiol. Lond.* 389: 187–203, 1987.

LANCASTER, B., NICOLL, R. A., AND PERKEL, D. J. Calcium activates two types of potassium channels in rat hippocampal neurons in culture. *J. Neurosci.* 11: 23–30, 1991.

LANG, D. G. AND RITCHIE, A. K. Large and small conductance calcium-activated potassium channels in the GH_3 anterior pituitary cell line. *Pfluegers Arch.* 410: 614–622, 1987.

LATORRE, R., VERGARA, C., AND HIDALGO, C. Reconstitution in planar lipid bilayers of a Ca^{2+}-dependent K^+ channel from transverse tubule membranes isolated from rabbit skeletal muscle. *Proc. Natl. Acad. Sci. USA* 77: 7484–7486, 1982.

LEE, K., ROWE, I. C. M., AND ASHFORD, M. L. J. Characterization of an ATP-modulated large conductance Ca^{2+}-activated K^+ channel present in rat cortical neurons. *J. Physiol. Lond.* 488: 319–337, 1995.

MAJOR, G., LARKMAN, A. U., JONAS, P., SAKMANN, B., AND JACK, J. J. Detailed passive cable models of whole-cell recorded CA3 pyramidal neurons in rat hippocampal slices. *J. Neurosci.* 14: 4613–4638, 1994.

MARTY, A. Ca-dependent potassium channel with large unitary conductance in chromaffin cell membranes. *Nature Lond.* 291: 497–500, 1981.

MARTY, A. The physiological role of calcium-dependent channels. *Trends Neurosci.* 12: 420–424, 1989.

MCCORMICK, D. A. AND PRINCE, D. A. Post-natal development of electrophysiological properties of rat cerebral cortical pyramidal neurons. *J. Physiol. Lond.* 393: 743–762, 1987.

MEECH, R. W. Intracellular calcium injection causes increased potassium conductance in *Aplysia* nerve cells. *Comp. Biochem. Physiol. A Comp. Physiol.* 42A: 493–499, 1972.

MEECH, R. W. Calcium-dependent potassium activation in nervous tissues. *Rev. Biophys. Bioeng.* 7: 1–18, 1978.

PALLOTA, B. S., MAGLEBY, K. L., AND BARRET, J. N. Single channel recordings in Ca^{2+}-activated K^+ currents in rat muscle cell culture. *Nature Lond.* 293: 471–474, 1981.

PAXINOS, G. AND WATSON, C. *The Rat Brain in Stereotaxic Coordinates.* Orlando, FL: Academic, 1986, p. 12–30.

REINHART, P. H., CHUNG, S., AND LEVITAN, I. A family of calcium-dependent potassium channels from rat brain. *Neuron* 2: 1031–1041, 1989.

REINHART, P. H., CHUNG, S., MARTIN, B. L., BRAUTIGAN, D. L., AND LEVITAN, I. B. Modulation of calcium-activated potassium channels from rat brain by protein kinase A and phosphatase 2A. *J. Neurosci.* 11: 1627–1635, 1991.

SAKMANN, B. AND NEHER, E. Geometric parameters of pipettes and membrane patches. In: *Single-Channel Recording,* edited by B. Sakmann and E. Neher. New York: Plenum, 1983, p. 45–46.

STOCKBRIDGE, N. EGTA. *Comput. Biol. Med.* 17: 299–304, 1987.

STORM, J. F. Action potential repolarization and a fast after-hyperpolarization in rat hippocampal pyramidal cells. *J. Physiol. Lond.* 365: 733–759, 1987.

TRAUTMAN, A. AND MARTY, A. Activation of Ca-dependent K channels by carbamoyl choline in rat lacrimal glands. *Proc. Natl. Acad. Sci. USA* 81: 611–615, 1984.

VOROBJEV, V. S. Vibrodissociation of sliced mammalian nervous tissue. *J. Neurosci. Methods* 38: 145–150, 1991.

WALSH, J. V. AND SINGER, J. J. Ca^{2+}-activated K^+ channels in vertebrate smooth muscle cells. *Cell Calcium* 4: 321–330, 1983.

WANN, K. T. AND RICHARDS, C. D. Properties of single calcium-activated potassium channels of large conductance in rat hippocampal neurons in culture. *Eur. J. Neurosci.* 6: 607–617, 1994.

WHITE, R. E., SCHONBRUNN, A., AND ARMSTRONG, D. L. Somatostatin stimulates Ca^{2+}-activated K^+ channels through protein dephosphorylation. *Nature Lond.* 351: 570–573, 1991.

WONG, R. K., PRINCE, D. A., AND BASBAUM, A. I. Intradendritic recordings from hippocampal neurons. *Proc. Natl. Acad. Sci. USA* 76: 986–990, 1979.

YELLEN, G. Ionic permeation and blockade in Ca^{2+}-activated K^+ channels of bovine chromaffin cells. *J. Gen. Physiol.* 84: 157–186, 1984.

YOSHIDA, A., ODA, M., AND IKEMOTO, Y. Kinetics of the Ca^{2+}-activated K^+ channel in rat hippocampal neurons. *Jpn. J. Physiol.* 41: 297–315, 1991.